Topoisomerase 1 inhibits MYC promoter activity by inducing G-quadruplex formation

Keller, Josephine Geertsen; Hymøller, Kirstine Mejlstrup; Thorsager, Maria Eriksen; Hansen, Noriko Y.; Erlandsen, Jens Uldum; Tesauro, Cinzia; Simonsen, Anne Katrine W.; Andersen, Anne Bech; Vandsø Petersen, Kamilla; Holm, Lise Lolle; Stougaard, Magnus; Andresen, Brage Storstein; Kristensen, Peter; Frøhlich, Rikke; Knudsen, Birgitta R.

Published in:
Nucleic Acids Research

DOI:
10.1093/nar/gkac482

Publication date:
2022

Document version:
Final published version

6332–6342 *Nucleic Acids Research, 2022, Vol. 50, No. 11* *Published online 10 June 2022*
https://doi.org/10.1093/nar/gkac482

Topoisomerase 1 inhibits *MYC* promoter activity by inducing G-quadruplex formation

Josephine Geertsen Keller[1,2], Kirstine Mejlstrup Hymøller[1], Maria Eriksen Thorsager[1], Noriko Y. Hansen[1], Jens Uldum Erlandsen[1], Cinzia Tesauro[1], Anne Katrine W. Simonsen[1], Anne Bech Andersen[1], Kamilla Vandsø Petersen[1], Lise Lolle Holm[3,4], Magnus Stougaard[2,5], Brage Storstein Andresen[3,4], Peter Kristensen[6], Rikke Frøhlich[1] and Birgitta R. Knudsen[1,*]

[1]Department of Molecular Biology and Genetics, Aarhus University, 8000 Aarhus C, Denmark, [2]Department of Clinical Medicine, Aarhus University, 8000 Aarhus C, Denmark, [3]Department of Biochemistry and Molecular Biology, University of Southern Denmark, 5230 Odense M, Denmark, [4]Villum Center for Bioanalytical Sciences, University of Southern Denmark, 5230 Odense M, Denmark, [5]Department of Pathology, Aarhus University Hospital, 8000 Aarhus C, Denmark and [6]Faculty of Engineering and Science, Department of Chemistry and Bioscience, Aalborg University, 9220 Aalborg, Denmark

Received January 28, 2022; Revised April 28, 2022; Editorial Decision May 23, 2022; Accepted June 07, 2022

ABSTRACT

We have investigated the function of human topoisomerase 1 (TOP1) in regulation of G-quadruplex (G4) formation in the Pu27 region of the *MYC* P1 promoter. Pu27 is among the best characterized G4 forming sequences in the human genome and it is well known that promoter activity is inhibited upon G4 formation in this region. We found that TOP1 downregulation stimulated transcription from a promoter with wild-type Pu27 but not if the G4 motif in Pu27 was interrupted by mutation(s). The effect was not specific to the *MYC* promoter and similar results were obtained for the G4 forming promoter element WT21. The other major DNA topoisomerases with relaxation activity, topoisomerases 2α and β, on the other hand, did not affect G4 dependent promoter activity. The cellular studies were supported by *in vitro* investigations demonstrating a high affinity of TOP1 for wild-type Pu27 but not for mutant sequences unable to form G4. Moreover, TOP1 was able to induce G4 formation in Pu27 inserted in double stranded plasmid DNA *in vitro.* This is the first time TOP1 has been demonstrated capable of inducing G4 formation in double stranded DNA and of influencing G4 formation in cells.

INTRODUCTION

Non-canonical four stranded G-quadruplex DNA structures (G4) are believed to play important biological functions (1–5). They have been the subject of intense studies since they were identified in cellular DNA by *in situ* immunostaining using the G4 specific single chain variable fragment (scFv), BG4 (6). However, their functions and regulations in living cells are far from fully elucidated.

G4 structures can form in specific G-rich sequences, the so-called G4 motifs, and appear as dynamic yet stable structural elements (5,7). G4 motifs are present throughout the human genome but are overrepresented in telomeric- and gene regulatory regions, for example promoters and 5′-UTRs (3,8). Of particular interest for human pathology, potential G4 motifs are frequently found in promoters of human proto-oncogenes such as *MYC, WT1*, *KRAS* and *TERT* (9–17). G4 formation has been confirmed in most of the promoters investigated (10–15) and available evidence suggests that they play an important role in the regulation of gene expression (10–13,15–17).

One of the best characterized G4 forming regions in human promoters is the Pu27 sequence that is part of the proto-oncogene *MYC* promoter (12). It is often used to study regulation of G4 formation in human cells (12,18,19). *MYC* has multiple promoters. Pu27 is part of the P1 promoter and more specifically located in the nuclease hypersensitive element III_1 ($NHEIII_1$) that controls 85–90% of *MYC* expression. Pu27 contains five G tracts and can fold into a parallel G4 structure that has an inhibitory effect on promoter activity (12,19).

*To whom correspondence should be addressed. Tel: +45 60202673; Email: brk@mbg.au.dk

Despite intense investigations during recent years, it is still poorly understood how G4 formation and resolution are controlled. From *in vitro* studies, it is known that G4 formation in at least single stranded DNA is influenced by the chemical composition of the surroundings. For example, G4 formation in synthetic oligonucleotides is destabilized by Li^+ and stabilized by K^+ or Na^+ (5,20). In a cellular context and in double stranded DNA, it is less clear how G4 formation is controlled. Cis-acting factors such as composition and sequence of bases clearly influence the transition between the G4 and the double stranded conformation of a given region (21,22). Consistently, several point mutations that reduce the G4 forming capability of the Pu27 region in the *MYC* promoter have been identified and verified *in vitro* and/or in cells using a reporter system in which a luciferase gene is placed under the control of the P1 promoter (12). DNA superhelicity appears to be another important factor in the regulation of G4 formation and footprinting studies have shown that G4 formation in double stranded DNA is stimulated by negative supercoils (21,23). It is likely the local unwinding of the DNA double helix associated with negative supercoiling that supports G4 formation, since G4 formation has been linked to R-loops in cells (24,25).

Several trans-acting proteins have also been demonstrated to influence G4 formation by the use of the above mentioned luciferase reporter system (19) as well as other methods. These proteins can roughly be separated into three subgroups based on the effect on G4. Proteins such as Rap1 and thrombin are inducers of G4 formation (26,27), while nucleolin and Ku are characterized as stabilizers (28,29). Finally, the RecQ helicases such as BLM, WRN, and SGS1 resolve G4 structures (30–32).

The nuclear enzyme human topoisomerase 1 (TOP1), may belong to the group of G4 influencing proteins. TOP1 is best known for its ability to regulate DNA topology during DNA metabolic processes such as transcription and replication (33–35). It relaxes positive and negative supercoils generated in front of and behind the tracking polymerase, respectively (33). Relaxation is accomplished by the enzyme introducing transient nicks in double stranded DNA, which allow the cleaved strand to rotate around the intact strand to remove torsional strain in the double helix. Hence, TOP1 may reduce G4 formation by removing negative supercoils. Moreover, a handful of studies have shown that purified TOP1 binds G4 structures with high affinity (36–39) and that the enzyme may even stimulate intermolecular G4 formation by a mechanism that depend on the active site tyrosine (39).

In the present study, we have addressed the function of TOP1 as a potential regulator of G4 in human promoters using Pu27 of the *MYC* promoter as a model G4 motif. We demonstrated that TOP1 downregulation in HEK293T cells stimulated transcription of a luciferase reporter gene under the control of $NHEIII_1$ with a wildtype Pu27 G4 motif but not when G4 formation in Pu27 was prevented by point mutation(s). Similar effects were not observed upon downregulation of the other major DNA human topoisomerases with relaxation activity, topoisomerase 2α (TOP2α) and topoisomerase 2β (TOP2β). The obtained data suggests that TOP1 inhibits promoter activity by directly inducing or stabilizing G4 formation in Pu27. This conclusion was supported by *in vitro* studies demonstrating a high affinity of TOP1 for the wildtype Pu27 sequence but not for a Pu27 derived sequence prevented in G4 formation by point mutations when inserted in single stranded oligonucleotides, as well as the ability of TOP1 to stimulate G4 formation in Pu27 inserted in double stranded plasmid DNA. TOP1 not only affected the *MYC* promoter but did also influence the activity of the G4 dependent WT21 promoter, suggesting a more general function of TOP1 in regulating G4 formation in human promoters.

MATERIALS AND METHODS

Oligonucleotides

All oligonucleotides were synthesized at Microsynth, Switzerland. The sequences of the oligonucleotides were as follows:

Pu27 5′-TGG GGA GGG TGG GGA GGG TGG GGA AGG-3′

Pu27(1(G/A)) 5′-TGG GGA GGG TGG GGA GAG TGG GGA AGG-3′

Pu27(5(G/A)) 5′-TGA GGA GAG TGA GGA GAG TGG AGA AGG-3′

Pu27 Scr 5′-AGA GTT GGG GGA TGG GGG GGG GGG GAG-3′

Pu27 Scr complementary 5′-CTC CCC CCC CCC CCA TCC CCC AAC TCT-3′

Pu27 forward PCR primer 5′-TTT ATA CTC ACA GGA CAA GG-3′

Pu27 reverse PCR primer 5′-GGA TGT AAA CAG AGT AAG AG-3′

Reagents, strains and antibodies

The del4 wildtype (#16604) and the pSang10-3F BG4 (#55756) plasmids were purchased from addgene, and the pRL-TK Renilla (#E2241) plasmid was purchased from Promega. The yeast *S. cerevisiae* strain RS190 lacking the endogenous TOP1 gene was a kind gift from R. Sternglanz (State University of New York, Stony Brook, NY). The plasmid pHT143, used for expression of TOP1, was described previously (40).

Rabbit anti-TOP1 (#A302-590A) and rabbit anti-TOP2α (#A300-054A) were purchased from Bethyl, mouse anti-TOP2β (#611493) from BD transduction, mouse anti-TBP (#ab818) from Abcam, and mouse anti-Lamin B (#sc-365214) were from Santa Cruz biotechnologies. All secondary antibodies were purchased from DAKO. siRNA targeting TOP1 (#3510923), TOP2α (#342786) and TOP2β (#3389257) as well as scrambled siRNA (#1027281) were from Qiagen, and the G4 drug PhenDC3 was from Sigma-Aldrich ApS.

Cell cultures

HEK293T cells were grown in Dulbecco's modified Eagle's medium (DMEM) supplemented with 10% fetal bovine serum (FBS), 100 units/ml penicillin and 100 μg/ml streptomycin (Sigma-Aldrich ApS). The cells were maintained in a humidified incubator (5% CO_2/95% air atmosphere at 37°C). When performing transfections, antibiotics were excluded from the medium.

Electronic mobility shift assay

10 pmol of 5′-Cy5 labelled oligonucleotide (OL_Pu27, OL_Pu27(1(G/A)), OL_Pu27(5(G/A))) were incubated with 0, 3, 9 or 18 pmol BG4 or 0, 1, 3 or 9 pmol TOP1 in G4 buffer (10 mM Tris–HCl, pH 7.5, 1 mM EDTA and 100 mM KCl) in a total volume of 30 μl for 30 min at 37°C. 5× DNA loading dye (20 mM Tris–HCl, pH 8, 60 mM EDTA, 60% glycerol, bromophenol blue) was added and the samples were loaded on a 12% native polyacrylamide gel (acrylamide:bis 37:5) and run at 4°C in 1xTBE (48 mM Tris, 45.5 mM boric acid, 1 mM EDTA) for 5 h at 170 V. The oligonucleotides were visualized on a Typhoon FLA 9500 scanner (GE Healthcare) at excitation 498 nm and emission 715 nm.

SPRi

Biotin 5′-end labelled oligonucleotides were diluted in 1× TBS (20 mM Tris, 150 mM NaCl) to 1 μM and immobilized on a gold SensEye G-strep chip (SSENS) by continuous flow in a CMF 2.0 Microfluidics spotter (Wasatch microfluidics) for 20 min, followed by a wash with TBST (20 mM Tris, 150 mM NaCl, 0.05% Tween-20) for 5 min. The sensor chip was transferred to the MX-96 SPR Imager (IBIS technologies), and the system was primed with SPRi buffer (10 mM Tris–HCl, pH 7.5, 1 mM EDTA, 100 mM KCl, 0.05% Tween-20). Residual background was blocked by injecting SPRi buffer supplemented with 20 mg/ml BSA for 10 min. To measure association kinetics, five or six injections of a 2-fold titration series ranging from 1.5625 to 200 nM protein were injected in sequence from the lowest to the highest concentration for 8 min, at a rate of 8 μl/s. Dissociation kinetics were measured by passing SPRi buffer over the chip for 6 min at a rate of 8 μl/s. The chip was regenerated with H_3PO_4 in between each protein concentration. A calibration curve was created by measuring SPRi response from dilutions of glycerol (ranging from 0 to 5%) in SPRi buffer and pure water as defined by the automated calibration routine of MX-96 SPR Imager. The program was run twice.

Data analysis: The SPRi data was imported into SprintX software (v. 2.1.1.0, IBIS technologies), calibrated, reference subtracted, and the baseline were zeroed. The starting time point was aligned at the beginning of each new injection. The data was collected in Scrubber (v. 2.0c, Biologics Inc.). Binding curves for all chip positions where binding was observed were fitted to the integrated rate equation to obtain association rate (K_a), dissociation rate (K_d) and equilibrium dissociation ($K_D = K_a/K_d$) constants. The simulations were calculated using ClampXP (v. 3.5, Biosensor Data Analysis). The data and simulations were exported in R (v. 3.5.3) to plot the resulting binding curves using ggplot2 (v. 3.2.1).

Luciferase assay

HEK293T cells were seeded in DMEM (10% FBS, no antibiotics) in a six-well plate and incubated overnight. After ∼24 h, transfection with plasmid DNA and siRNA was performed. Cells were transfected with 2 μg of del4 wild-type or mutated plasmid, 0.5 μg pRL-TK Renilla plasmid and a 1:1:1:1 mixture of siRNA against TOP1 (HS TOP1 #3510923 GeneSolution Qiagen), TOP2α (HS TOP2α #342786 GeneSolution Qiagen), TOP2β (HS TOP2β #3389257GeneSolution Qiagen) or scrambled siRNA (All-Stars Negative Control siRNA #1027281, Qiagen). 72 h after transfection, dead cells and cell debris were removed by two times wash with PBS before the remaining cells were trypsinated. 4000 transfected cells were seeded in a 96-well plate in 50 μl DMEM (10% FBS, no antibiotics). 50 μl Dual-Glo Luciferase Reagent (Promega) was added and the cells were incubated 10 min at room temperature before the firefly luminescence of the cells was measured using Fluostar Optima (BMG Labtech) with settings on 0.2 s positioning delay, 0.0 s measurement start time and 0.1 s as the interval. This was followed by addition of 50 μl Dual-Glo Stop & Glo (Promega), and the cells were left for additional 10 min of incubation at room temperature before the renilla luminescence was measured using the same settings.

BG4 immunoprecipitation

83 fmol plasmid was mixed with 4150 fmol BG4 in G4 buffer (10 mM Tris–HCl pH 7.5, 1 mM EDTA, 100 mM KCl) in a total volume of 100 μl. The samples were incubated 30 min at 37°C and added to His-Tag Isolation and Pulldown Dynabeads (ThermoFisher) that were pre-blocked with 1 mM dNTP overnight at 4°C. The samples were incubated additional 10 min at room temperature. The beads were collected and washed 4 times with 100 μl G4 buffer. Bound plasmid was eluted by the addition of 1× TE (10 mM Tris–HCl pH 7.5, 0.1 mM EDTA) supplemented with 1% SDS and 10 mg/ml Proteinase K and incubated at 37°C for 30 min. The samples were EtOH precipitated overnight, and the pellet was resuspended in 1× TE and used as a template for Taq PCR using Pu27 forward and reverse PCR primers. The PCR samples were run on a 1.5% agarose gel with SYBR safe for 1 h at 65 mA.

BG4 immunoprecipitation with TOP1. Supercoiled plasmid was linearized before addition of purified TOP1.

2 μg del4_Pu27, del4_Pu27(1(G/A)), and del4_Pu27(5(G/A)) was incubated individually with 20 units of the single cutter EcoRI in reaction buffer (50 mM K-acetate, 20 mM Tris-acetate, 10 mM Mg-acetate, 100 μg/ml BSA, pH 7.9). After 1 h incubation at 37°C the samples were heat inactivated at 65°C for 20 min, and the linearization was confirmed by running the DNA on a 1% agarose gel. The linearized DNA was ligated overnight at 16°C by T4 ligase and subsequently EtOH precipitated.

300 ng relaxed plasmid was incubated with purified TOP1 or TOP1 storage buffer (10 mM Tris–HCl pH 7.5, 1 mM EDTA, 313 mM NaCl, 50% glycerol) in G4 buffer in a total volume of 100 μl. The samples were incubated at 37°C for 30 min before 4150 fmol BG4 was added. The samples were then immunoprecipitated as described above.

Plasmid DNA relaxation

400 pmol oligonucleotide (OL_Pu27, OL_Pu27(1(G/A)), OL_Pu27(5(G/A)) or OL_dsSCR) was mixed with 5× relaxation buffer (50 mM Tris–HCl, pH 7.5, 25 mM $MgCl_2$,

25 mM $CaCl_2$, 685 mM KCl) followed by addition of 200 fmol supercoiled pUC18 plasmid. The samples were incubated 5 min at 37°C. The relaxation was initiated by the addition of purified TOP1, and the samples were incubated at 37°C for increasing timepoints as indicated in the figure legend. The reactions were stopped with 0.1% SDS and subsequently mixed with 10 mg/ml Proteinase K followed by incubation for 1 h at 37°C. DNA loading buffer (24 mM Tris, 22.75 mM boric acid, 0.5 mM EDTA, 25% glycerol, xylene cyanol, bromophenol blue) was added to the samples, and they were run on a 1% agarose gel without dye for 12 h at 30V, 4°C. The gel was stained with EtBr for 30 min and subsequently destained in 1× TBE (48 mM Tris, 45.5 mM Boric Acid, 1 mM EDTA) for 20 min.

RESULTS

Downregulation of TOP1 influences G4 regulated *MYC* expression

As mentioned in the introduction, TOP1 has been shown to bind G4 structures in synthetic oligonucleotides with high affinity (37–39), and it was even suggested that the enzyme introduces intermolecular G4 structures in synthetic DNA *in vitro* (39). It can therefore be speculated that TOP1 may play an *in vivo* role in regulating G4 formation. Thereby it may affect transcription from promoters with confirmed G4 forming sequences.

To address this possibility, we have used a previously developed luciferase reporter assay (12) to monitor the promoter activity of the *MYC* $NHEIII_1$, since the activity of this promoter element is known to be inhibited by G4 formation in the G4 motif, Pu27 (12,19). As negative controls we used promoter elements with mutations that destabilize G4 formation. The utilized reporter plasmids, termed del4, with wildtype or mutated Pu27 regions are illustrated in Figure 1A. They all contain a truncated *MYC* promoter containing the promoter elements P1 (including $NHEIII_1$) and P2 inserted in front of the luciferase reporter gene firefly. Promoter activity was monitored by measuring the activity of firefly relative to the activity of luciferase renilla. The renilla gene was inserted under the control of a constitutive promoter in a plasmid co-transfected with del4 to allow for normalization of different transfection efficiencies as described in (12).

Based on the literature, we chose as one negative control to use a del4 variant with a single base substitution (G257A) in the Pu27 region, named del4_Pu27(1(G/A)) (previously termed del4 dual (12)). This mutation has previously been demonstrated to inhibit G4 formation and increase transcription from the $NHEIII_1$ promoter element (12). However, our circular dichroism (CD) analysis indicated that the mutation G257A in Pu27 is insufficient to prevent G4 formation in single stranded oligonucleotides (Supplementary Figure S1A). We therefore included an additional del4 negative control with five base substitutions in Pu27 (G252A, G257A, G262A, G266A, G271A) named del4_Pu27(5(G/A)), to fully prevent G4 formation. The inability of an oligonucleotide with this sequence to form a G4 structure was confirmed by CD analysis (see Supplementary Figure S1A). Also, the G4 forming capability of the oligonucleotides OL_Pu27 and OL_Pu27(1(G/A)) but not OL_Pu27(5(G/A)) was confirmed by their relative gel-electrophoretic mobility with the two formers showing an increased mobility relative to OL_Pu27(5(G/A)). The increased mobility is an indication of a more compact structure consistent with G4 formation (Supplementary Figure S1B).

To further address the G4 forming capacities of the wildtype, 1(G/A), and 5(G/A) Pu27 sequences, we investigated the affinity of the purified anti-G4 scFv, BG4, (6) (see Supplementary Figure S2 for purity of BG4) for synthetic oligonucleotides with these sequences. This was done by electrophoretic mobility shift assays (EMSA) and by surface plasmon resonance imaging (SPRi). EMSA analysis demonstrated the retardation (marked with an asterisk) of 5′-Cy5 labelled oligonucleotides with the wildtype Pu27 sequence (OL_Pu27) or with a single G257A base substitution in the Pu27 sequence (OL_Pu27(1(G/A))) upon incubation with BG4 (Figure 1B, compare lanes 2–4 with lane 1 and lanes 6–8 with lane 5). The mobility of the oligonucleotide with all five base substitutions in the Pu27 sequence (OL_Pu27(5(G/A))) was unaffected by addition of BG4 (compare lanes 10–12 with lane 9). This result further supports the G4 forming capacity of OL_Pu27 and OL_Pu27(1(G/A)) but not OL_Pu27(5(G/A)). Next, we analyzed BG4 binding to the different Pu27 derived sequences with SPRi. For these studies, 5′-biotin labeled OL_Pu27, OL_Pu27(1(G/A)) and OL_Pu27(5(G/A)) were coupled to a streptavidin functionalized sensor chip. The exposure to increasing concentrations of BG4 ranging from 6.25 nM to 200 nM were analyzed (Figure 1C). The resulting binding curves demonstrated a pronounced decrease in binding of BG4 to OL_Pu27(5(G/A)), which is in agreement with the results of EMSA. This was also reflected by the calculated KD values of 166 and 246 nM for BG4 binding to OL_Pu27 and OL_Pu27(1(G/A)), and 7948 nM for BG4 binding to OL_Pu27(5(G/A)). Taken together, the *in vitro* experiments demonstrated the capability of Pu27 and Pu27(1(G/A)), but not Pu27(5(G/A)) to form a G4 structure when inserted in single stranded DNA.

The effect of TOP1 on transcription controlled by $NHEIII_1$ with wildtype Pu27, Pu27(1(G/A), or Pu27(5(G/A)) was investigated using the luciferase reporter system as described (12). HEK293T cells with or without siRNA mediated downregulation of TOP1 expression were transfected with either one of the reporter plasmids (del4_Pu27, del4_Pu27(1(G/A)), del4_Pu27(5(G/A))) and the luciferase expression was measured following manufactures protocol (Figure 2). It was not possible to perform sequential transfection of reporter plasmids and siRNA due to substantial cell death after two transfections. Therefore, the cells were transfected simultaneously with plasmids and siRNA. Downregulation of TOP1 was confirmed by Western blotting to ∼85% reduction of TOP1 protein level at the timepoint (72 h post transfection) where promoter activity was measured (Supplementary Figure S3A), and already 48 h post transfection we observed a >50% downregulation of TOP1 (Supplementary Figure S3A). Hence, we were able to confirm markedly reduced TOP1 protein levels well before and at the time where the experiment was performed. The luciferase reporter assay shows that the 1(G/A) mutation enhanced promoter

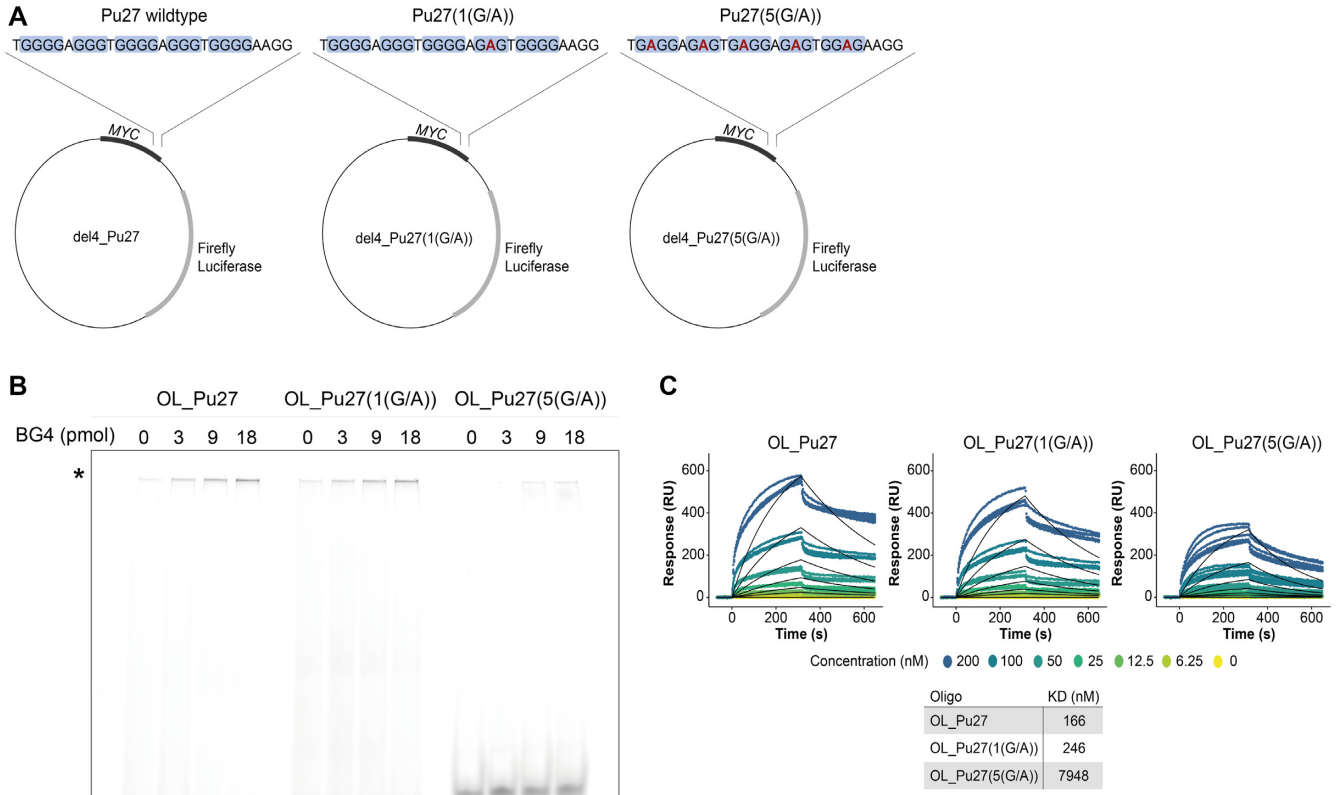

Figure 1. (**A**) The reporter plasmids, named del4, containing a wildtype or mutated Pu27 region. The mutated del4 plasmids contained either a single or five G to A base substitutions and are named del4_Pu27(1(G/A)) or del4_Pu27(5(G/A)). (**B**) EMSA showing the mobility of the wildtype Pu27 oligonucleotide (OL_Pu27) (lanes 1-4) or the two mutant oligonucleotides, (OL_Pu27(1/G/A)) (lanes 5-8) and OL_Pu27(5(G/A)) (lanes 9–12)) after incubation with 0, 3, 9 or 18 pmol of BG4. Gel electrophoretic retarded products are marked by an asterisk. (**C**) The top panel shows a representative example of the SPRi binding curves obtained when presenting increasing concentration of BG4 for OL_Pu27, OL_Pu27(1(G/A)), or OL_Pu27(5(G/A)). The lower panel shows the equilibrium dissociations constants (K_D) calculated from three independent experiments.

activity compared to transcription under control of the wildtype $NHEIII_1$ sequence in cells with normal TOP1 expression (shown as grey bars). This result is consistent with the literature (12) suggesting that the G257A base substitutions in Pu27 is sufficient to destabilize G4 formation in cells leading to an increase in transcription activity. The promoter activity in del4_Pu27(5(G/A) that contains five base substitutions in the Pu27 region sufficient to destabilize G4 formation even in single stranded DNA (see above), was not enhanced compared to the promoter activity in del4_Pu27. This may reflect that the five base substitutions in top of preventing G4 formation, inhibited binding to positive acting transcription factors such as SP1, heterogenous nuclear ribonucleoprotein K (hnRNP K) and CCHC-type zinc finger nucleic acid binding protein (CNBP), leading to a reduced transcription level (41).

TOP1 downregulation was associated with a dramatic increase in the promoter activity of the $NHEIII_1$ with wildtype Pu27, to a level even above the activity of G4 compromised $NHEIII_1$ Pu27(1(G/A)). Transcription under the control of $NHEIII_1$ Pu27(1(G/A)) or $NHEIII_1$ Pu27(5(G/A)), on the other hand, was unaffected by TOP1 downregulation (compare the blue bars of Figure 2). Consistent with the ability of the wildtype but not the mutated $NHEIII_1$ promoter elements to form G4 structures, the G4 stabilizing ligand PhenDC3 inhibited transcription only from the wildtype $NHEIII_1$ and not from the mutated variants hereof (Supplementary Figure S4). Hence, the increased transcription from $NHEIII_1$ Pu27 and not $NHEIII_1$ Pu27(1(G/A)) or $NHEIII_1$ Pu27(5(G/A)) upon TOP1 downregulation is in concordance with TOP1 playing a central role in stabilizing or inducing G4 formation in the *MYC* promoter in cells. This was further supported by the finding that downregulation of TOP1 resulted in increased transcription of endogenous *MYC* as demonstrated by qPCR analysis (Supplementary Figure S5). Moreover, the ability of TOP1 to influence transcription from promoters with G4 forming regions was not restricted to the *MYC* promoter. Hence, TOP1 downregulation resulted in a pronounced stimulation of transcription from the previously

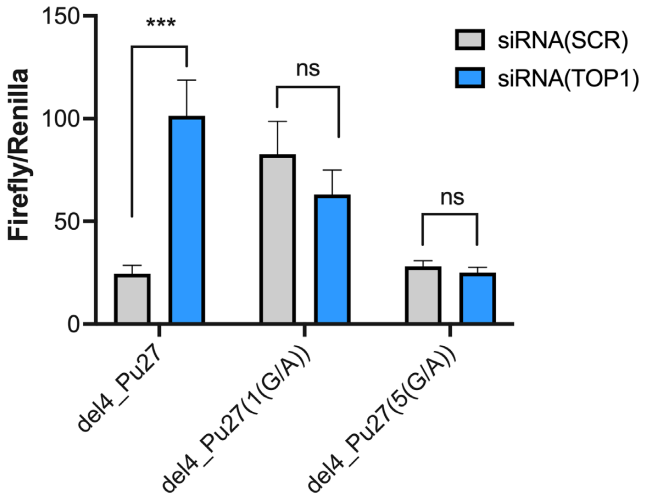

Figure 2. Quantitative depiction of the Pu27 promoter activity measured in terms of luciferase expression after treatment with equal concentrations of scrambled siRNA (grey bars) or TOP1 targeting siRNA (blue bars). Plotted data represent average +/− standard error of the mean, $n = 9$. *** indicates significant difference, $P < 0.001$; ns, non-significant difference. Unpaired *t*-test with Welch's correlation.

described G4 forming WT21 promoter region (13,42) when the G4 motif of this region was intact but not when G4 formation was prevented by mutations (Supplementary Figure S6).

The effect of TOP1 on G4 formation in Pu27 and mutants hereof

To address if the TOP1 dependent activity of the $NHEIII_1$ promoter could be ascribed to regulation of G4 formation, we investigated if the effect of TOP1 could be correlated to the ability of Pu27 or its mutants to form G4 structures when inserted in plasmid DNA.

First, we addressed if the del4 plasmid harbors G4 motifs in other regions than Pu27. For this purpose, we performed an *in silico* analysis using the G4 hunter tool previously described by Brázda *et al.* (43). Setting the window size at 25 nucleotides and the threshold score at 1.2 (based on (43)), we identified 12 putative G4 motifs in the del4 plasmid backbone outside the $NHEIII_1$ region. However, none of these sequences could form G4 structures when present in single stranded synthetic DNA as demonstrated by CD analysis (Supplementary Figure S7). We therefore went on and investigated G4 structure formation in the wildtype Pu27, Pu27(1(G/A)) or Pu27(5(G/A)) of the del4 plasmids by using immunoprecipitation with BG4. Each of the three plasmids were incubated with 6xHis tagged BG4 in a K^+ containing buffer before pulldown by BG4 with 6xHis affinity magnetic beads functionalized with Co^{2+}. Figure 3A shows a representative example of the products formed after 20 cycles of PCR amplification of the del4_Pu27, del4_Pu27(1(G/A)), or del4_Pu27(5(G/A)) that co-immunoprecipitated with BG4 from equal concentrations of input plasmids. Only del4_Pu27 and neither of the mutated plasmids co-immunoprecipitated with BG4 (see lanes 1, 3 and 5). This indicates the presence of a G4 structure in the del4_Pu27 plasmid but not in the two mutated plasmids. Since the three plasmids were identical except for the Pu27 region, the result is consistent with the plasmids being unable to form G4 in sequences outside the Pu27. The precipitation of del4_Pu27 was clearly dependent on the addition of BG4. Only trace amount of PCR products, probably resulting from a weak unspecific plasmid-to-bead interaction, were generated in samples without added BG4 (lanes 2, 4 and 6). The results of the immunoprecipitation experiments demonstrate the presence of a G4 structure in the del4_Pu27 and the absence of such structure in the two mutated plasmids. This result correlates with the differences between del4_Pu27 and the two mutated plasmids observed in Figure 2 and supports the notion that G4 formation inhibits the promoter activity of $NHEIII_1$.

A putative direct effect of TOP1 on G4 formation was addressed in a co-immunoprecipitation experiment as the one described under Figure 3A with or without added purified TOP1 (see Supplementary Figure S2 for purity of TOP1). Plasmids purified from bacteria are negatively supercoiled, and negative supercoils support G4 formation (21,22). The addition of TOP1 will rapidly relax plasmids, which in turn may affect G4 formation and influence the result. To avoid putative artifacts caused by the relaxation activity of TOP1, the plasmids were relaxed by linearization with a restriction endonuclease (Supplementary Figure S8). Subsequently, they were incubated with TOP1 and 6xHis tagged BG4. Co-immunoprecipitation showed that significantly more PCR product was obtained after co-immunoprecipitation of del4_Pu27 in the presence of TOP1 compared to the negative control without added TOP1 (Figure 3B). This suggests that TOP1 may induce G4 formation in Pu27. The same tendency was observed when precipitating del4_Pu27(1(G/A)) in the absence or presence of TOP1 (lanes 3 and 4), although less pronounced as for del4_Pu27. The amount of immunoprecipitated del4_Pu27(5(G/A)) appeared to be at background levels both when precipitated from samples with or without added TOP1 (lanes 5 and 6), and we observed no significant differences between the two samples (see the graphical depiction). Hence, at the utilized assay conditions TOP1 appears capable of inducing G4 formation in del4_Pu27 and to a lesser extent in del4_Pu27(1(G/A)) but not in del4_Pu27(5(G/A)). Since the only difference between del4_Pu27(5(G/A)) and the two other plasmids is the sequence of Pu27, this result strongly suggests that the G4 structure induced by TOP1 is the one formed in Pu27.

TOP1 binds G4 structures

The results shown in Figure 3B indicate that TOP1 can induce G4 structures in relaxed double stranded DNA. This may explain the inhibitory effect of TOP1 on transcription from the G4 forming *MYC* promoter element $NHEIII_1$ as shown in Figure 2. TOP1 may be directly involved in regulating G4 formation. The enzyme may also play a more indirect role since G4 structure formation is largely affected by topological tension in the DNA and since TOP1 is an important cellular regulator of DNA topology (33–35). To address this possibility, we measured $NHEIII_1$ promoter activity (as described under Figure 2) in HEK293T cells with or without downregulation of either of the two other

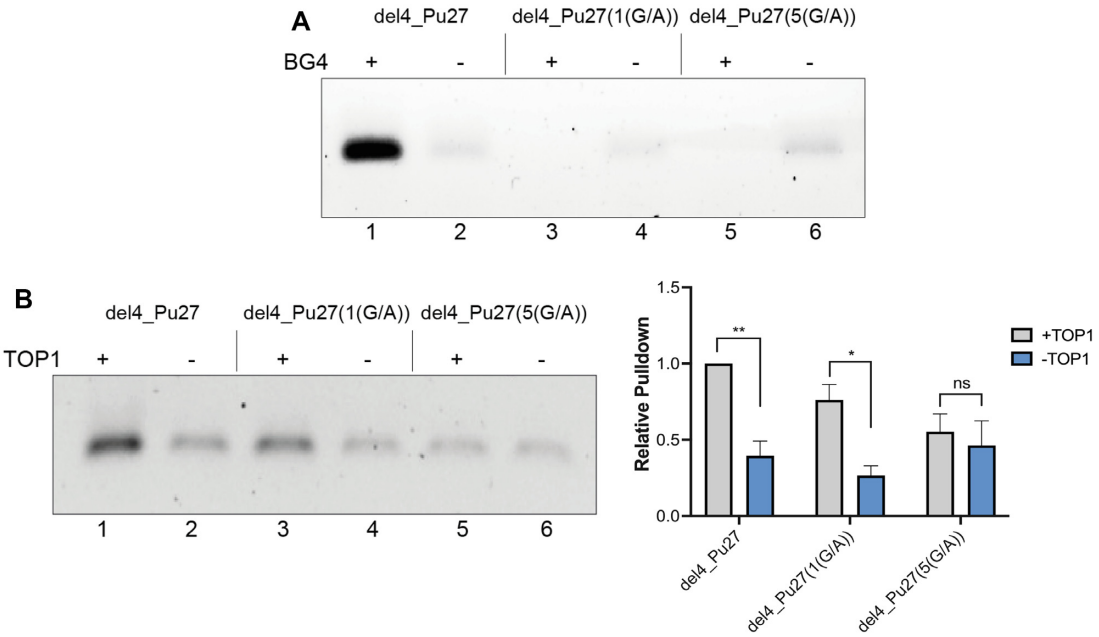

Figure 3. (**A**) The del4 plasmids, del4_Pu27 (lanes 1-2), del4_Pu27(1(G/A)) (lanes 3-4) and del4_Pu27(5(G/A)) (lanes 5 and 6) were incubated with or without 6xHis-tagged BG4 and pulled down with Co^{2+} functionalized magnetic beads as indicated in top of the gel-picture. The gel picture shows the result of 20 cycles PCR amplification of pulled down plasmids analyzed in a 1% agarose gel. (**B**) Linearized del4 plasmids, del4_Pu27 (lanes 1 and 2), del4_Pu27(1(G/A)) (lanes 3 and 4) and del4_Pu27(5(G/A)) (lanes 5 and 6) were incubated with or without TOP1 as indicated in top of the gel picture and subsequently immunoprecipitated with BG4 as described under A. The gel picture shows the result of PCR amplification of pulled down plasmid DNA as described under A. The right panel is a graphical depiction of quantifying the PCR products obtained in five independent experiments. Plotted data represent average ± standard error of the mean, $n = 5$. * indicates significant difference, * $P < 0.05$; ** $P < 0.005$; ns, non-significant difference. Unpaired *t*-test with Welch's correlation. Band intensities were quantified by using ImageJ.

major DNA relaxing human topoisomerases, TOP2α and TOP2β. TOP2α and TOP2β protein levels were reduced by approximately 80% and 90%, respectively, by siRNA treatment (Supplementary Figure S9) measured 72 h post transfection at which time the promoter activity was measured using the luciferase reporter system (Figure 4). Note, that at these conditions a substantial part of cells with knockdown of the life essential TOP2α enzyme died. However, these were removed before promoter activity was measured as described under materials and methods. As evident from Figure 4A, downregulation of TOP2α had no effect on the activity of neither the wildtype $NHEIII_1$ nor the G4 compromised $NHEIII_1$ promoter elements. This is consistent with previous studies, which suggest that TOP2α is primarily involved in decatenation of interlinked sister chromatids during replication termination rather than relaxation of supercoils *per se* (44). Downregulation of TOP2β, on the other hand, resulted in an increased promoter activity of both the wildtype and the mutated $NHEIII_1$ promoter elements (see Figure 4B). The $NHEIII_1$ promoter element contains several strong TOP2 cleavage sites (45). To our knowledge it is not investigated if these sites are preferentially cleaved by TOP2β, and we have no knowledge of evidence that can explain the increased transcription from the $NHEIII_1$ promoter upon TOP2β downregulation. However, the altered expression pattern upon TOP2β downregulation is markedly different than after TOP1 downregulation and appears independent on the G4 capability of $NHEIII_1$. Since TOP2β and TOP1 combined represent the major cellular DNA relaxation activities, the results argue against G4 regulated transcription being affected primarily by dysregulated DNA topology upon TOP1 downregulation and for a more direct role of TOP1 in G4 formation.

It has been reported that TOP1 has a high affinity for G4 structures (37–39) and it is possible that the enzyme induces G4 formation via direct interaction (39). The binding of TOP1 to the wildtype or mutated Pu27 sequences used in the present study was investigated in a standard competition experiment. This was done by measuring the relaxation activity of TOP1 in the absence or presence of equal concentrations of competitor oligonucleotides with the relevant sequences. The sequences of the competitor DNAs are shown in Figure 5A and include three 27-mers with the sequence of wildtype Pu27, Pu27(1(G/A)), Pu27(5(G/A)) as well as a 27 bp double stranded DNA fragment with a scrambled sequence (OL_dsSCR) with the same G content as Pu27 in one strand. In the experimental setup, TOP1 was incubated with negatively supercoiled pUC18 and 400 pmol of each of the competitors for increasing time intervals as indicated in Figure 5B, before the reactions were terminated and analyzed in a 1% agarose gel. The unreacted supercoiled plasmid (marked SC) that act as a substrate for TOP1 relaxation is highly condensed and migrates fast in the gel, while the relaxed product (marked R) migrates slower. As evident from the gel picture, TOP1 converted all supercoiled plasmid to relaxed forms within 7 s without added competitor (compare lanes 1 and 2). The same relaxation pattern was observed upon addition of the OL_Pu27(5(G/A)) competitor (compare lanes 18–22 with lanes 2–6), while a modest reduction in the TOP1 relaxation rate was observed upon ad-

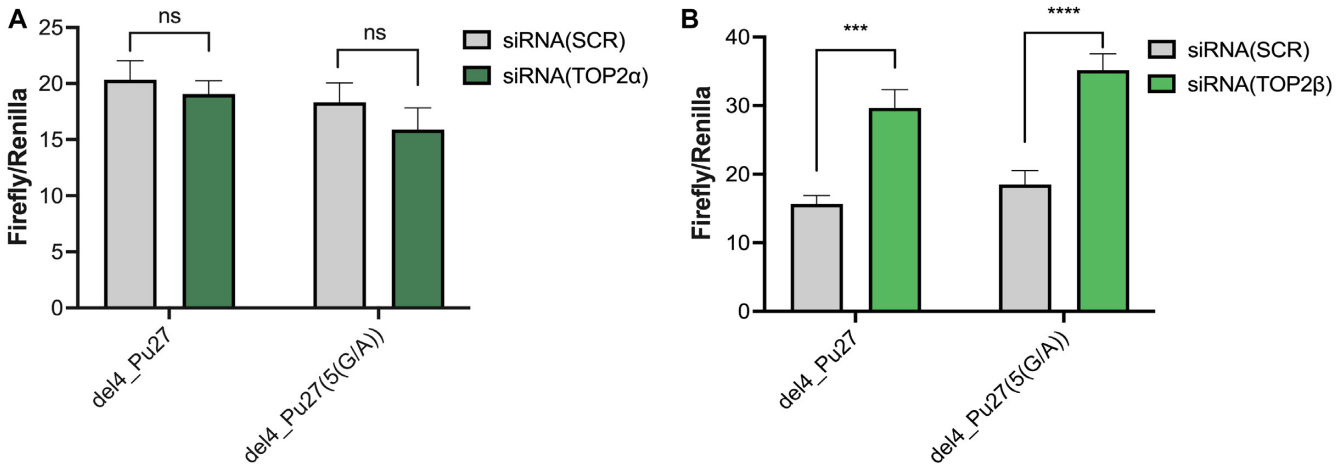

Figure 4. (**A**) Quantitative depiction of the Pu27 promoter activity measured in terms of luciferase expression after treatment with scrambled siRNA (grey bars) or siRNA targeting TOP2α (green bars). (**B**) same as (A), except that the green bars represent cells treated with siRNA targeting TOP2β. Plotted data represent average ± standard error of the mean, $n = 15$. * indicates significant difference, ***$P < 0.001$, ****$P < 0.0001$; ns, non-significant difference. Unpaired *t*-test with Welch's correlation.

dition of OL_Pu27(1(G/A)) or OL_dsSCR (compare lanes 13–17 and 23–27 with 2–6). In contrast, the addition of the wildtype Pu27 competitor resulted in a pronounced inhibition of TOP1 relaxation and full relaxation of the plasmid was not achieved within the duration of the experiment (lanes 7–12). This result is in accordance with previous studies (36–38) and indicates a high binding affinity of TOP1 for the G4 forming Pu27 sequence compared to the dsSCR that represent a natural double stranded substrate of TOP1.

The high affinity of TOP1 for G4 was confirmed by EMSA obtained by incubating 5′-Cy5 labeled OL_Pu27, OL_Pu27(1(G/A)) or OL_Pu27(5(G/A)) with 0-9 pmol TOP1 before analysis in a 12% native polyacrylamide gel. The result shown in Figure 5C demonstrates retardation of OL_Pu27, and OL_Pu27(1(G/A)) (marked with asterisk) and not OL_Pu27(5(G/A)). Likewise, TOP1 bound OL_Pu27 and OL_Pu27(1(G/A)) with high affinity when analyzed by SPRi, while no binding to OL_Pu27(5(G/A)) was observed (Figure 5D).

DISCUSSION

Using the luciferase reporter system (12), we demonstrated that TOP1 downregulation in HEK293T cells resulted in a significantly increase in the activity of a truncated *MYC* promoter containing a $NHEIII_1$ region with a wildtype Pu27 G4 motif, but not when the G4 motif was altered by one or five G to A base substitutions (Pu27(1(G/A)) or Pu27(5(G/A))). In agreement with previous studies (12) these results supported that the change in promoter activity was G4 dependent. This is consistent with the finding that the G4 stabilizing ligand PhenDC3 inhibited the activity of $NHEIII_1$ with wildtype Pu27 but not $NHEIII_1$ with Pu27(5(G/A)). The results suggest a role of TOP1 in stimulating or stabilizing G4 formation in cells. This was further supported by another G4 forming promoter element (WT21) being regulated by TOP1 in a similar manner as Pu27, and by TOP1 downregulation stimulating expression of the endogenous *MYC* gene.

BG4 immunoprecipitation of negatively supercoiled del4_Pu27, del4_Pu27(1(G/A)) and del4_Pu27(5(G/A)) reporter plasmids demonstrated pulldown of the plasmid containing wildtype Pu27 but not of plasmids containing the mutated forms of Pu27. This result strongly indicates the presence of a G4 structure in del4_Pu27 but not in del4_Pu27(1(G/A)) and del4_Pu27(5(G/A)). Interestingly the ability of plasmid DNA and oligonucleotides with the wildtype or mutated Pu27 G4 motifs to form G4 varied markedly as evident when comparing the results of EMSA and CD analysis with the results of immunoprecipitation of plasmid DNA. Hence, the oligonucleotide with the Pu27(1(G/A)) sequence that was unable to form G4 in the supercoiled plasmid, showed a G4 characteristic CD spectra similar to the oligonucleotide with a wildtype Pu27 sequence and was retarded by BG4 in EMSA. Only the Pu27(5(G/A)) sequence was prevented from G4 formation when present in a single stranded oligonucleotide form. When present in relaxed double stranded DNA, on the other hand, neither of the Pu27 derived sequences appeared capable of forming G4 structures as evident from the result of immunoprecipitation of linearized del4 plasmids with BG4. This supports the stimulatory effect of negative supercoils on G4 formation in double stranded DNA. The observed differences highlight the different abilities of single or double stranded DNA, with different superhelicity, to support G4 formation. This emphasizes the importance of considering the composition of DNA model systems when addressing biological relevant questions involving G4 structures.

BG4 immunoprecipitation experiments of relaxed plasmid DNA with or without addition of purified TOP1 demonstrated the ability of the enzyme to induce G4 formation in the wildtype Pu27 sequence *in vitro*. G4 was not induced by TOP1 in the Pu27(5(G/A)) sequence and to a lesser extend in the Pu27(1(G/A)) sequence. This result suggests that the single point mutation in the Pu27 G4 motif is not sufficient to completely block the G4 forming potential of the sequence, which is in agreement with the G4

A

Oligo name	Sequence
OL_Pu27	5′-TGG GGA GGG TGG GGA GGG TGG GGA AGG
OL_Pu27(1(G/A))	5′-TGG GGA GGG TGG GGA GAG TGG GGA AGG
OL_Pu27(5(G/A))	5′-TGA GGA GAG TGA GGA GAG TGG AGA AGG
OL_dsSCR	5′-AGA GTT GGG GGA TGG GGG GGG GGG GAG 3′-TCT CAA CCC CCT ACC CCC CCC CCC CTC

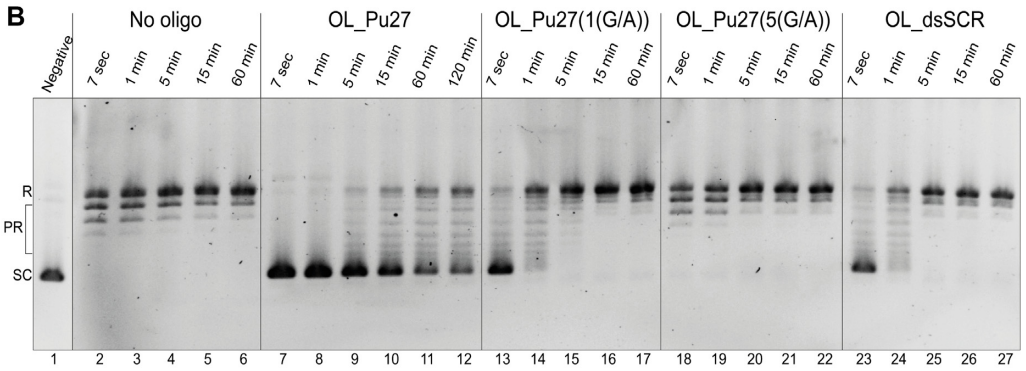

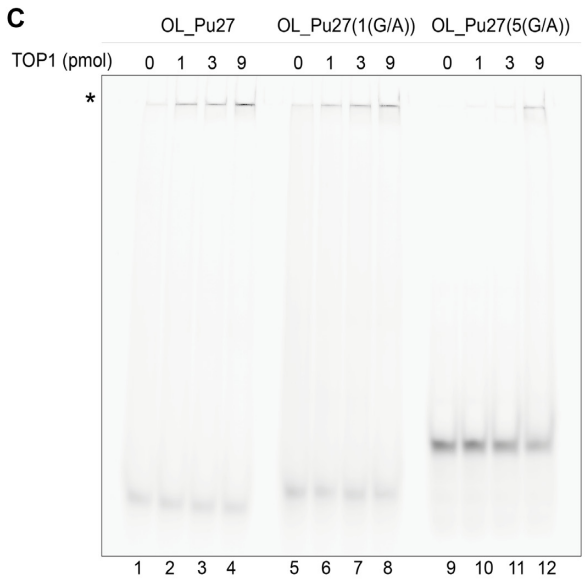

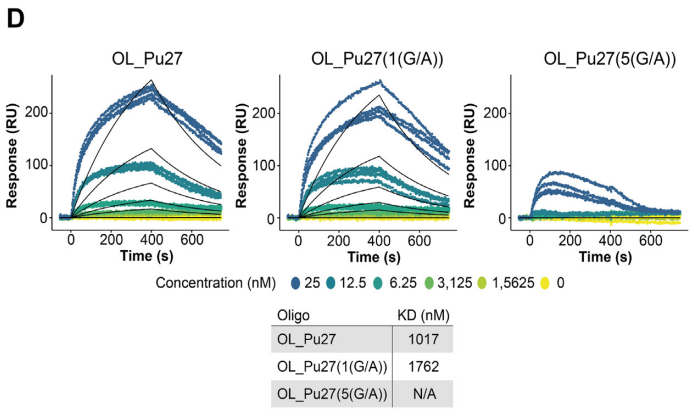

Oligo	KD (nM)
OL_Pu27	1017
OL_Pu27(1(G/A))	1762
OL_Pu27(5(G/A))	N/A

Figure 5. (**A**) Sequences of OL_Pu27, OL_Pu27(1(G/A)), OL_Pu27(5(G/A)) and OL_dsSCR. (**B**) The result of DNA relaxation for increasing time intervals with 2 pmol TOP1 in the absence of added oligonucleotide competitor DNA (lanes 2-6) or in the presence of 400 pmol of OL_Pu27 (lanes 7-12), OL_Pu27(1(G/A)) (lanes 13–17), OL_Pu27(5(G/A)) (lanes 18–22) or OL_dsSCR (lanes 23–27). Lane 1 is a control containing plasmid DNA incubated without TOP1. The identity of the products is indicated to the left of the picture. SC; supercoiled plasmid, R; relaxed plasmid. PR; partly relaxed plasmid. (**C**) EMSA showing the mobility of the wildtype Pu27 oligonucleotide (OL_Pu27) (lanes 1–4) or the two mutants (OL_Pu27(1/G/A)) (lanes 5–8) and OL_Pu27(5(G/A)) (lanes 9–12)) after incubation with 0, 1, 3 or 9 pmol of TOP1. Retarded products are marked by an asterisk. (**D**) The top panel shows a representative example of SPRi binding curves obtained when presenting increasing concentration of TOP1 for OL_Pu27, OL_Pu27(1(G/A)) or OL_Pu27(5(G/A)). The lower panel shows the equilibrium dissociations constants (K_D) calculated from three independent experiments.

characteristic CD spectra observed when analyzing a single stranded oligonucleotide with this sequence.

The ability of TOP1 to induce G4 formation in relaxed del4_Pu27 is consistent with the enhanced activity of the wildtype $NHEIII_1$ promoter element observed in HEK293T cells upon TOP1 downregulation. In contrast, the activities of $NHEIII_1$ with either of the mutated Pu27 sequences were unaffected by TOP1 downregulation, suggesting that TOP1 may be unable to stimulate G4 formation in both Pu27(1(G/A)) and Pu27(5(G/A)) when present in a cellular context. The reason for this discrepancy remains unclear. However, one explanation may be the presence of G4 resolving transacting factors such as for example RecQ helicase family members (WRN and BLM)

(30,31) present in cells but not in the cell free experimental setup.

The pulldown of linearized del4 plasmids with BG4 suggested that TOP1 induces G4 structure formation in the Pu27 G4 motif in a topology independent manner possibly via a direct interaction. This is consistent with the previously reported ability of wildtype TOP1 or a N-terminal truncated mutant to induce intermolecular G4 formation in oligonucleotides (39). Also it was supported by the classical competition experiment in which OL_Pu27 markedly reduced the relaxation activity of purified TOP1 indicating a strong affinity of TOP1 to G4, which is consistent with previous findings (36–39). In comparison, the inhibitory effect of OL_Pu27(1(G/A)) was more modest and equal to that of a double stranded DNA fragment with similar length and G content in one of the strands as the Pu27 sequence. Relaxation was unaffected by addition of OL_Pu27(5(G/A)). These results were in agreement with EMSA and SPRi analyses demonstrating the highest affinity of TOP1 to OL_Pu27, a weakened affinity to OL_Pu27(G1(G/A)), and no binding to OL_Pu27(G5(G/A)).

All experiments performed in a cell free environment suggested that TOP1 binds to and induces G4 formation in a topology independent manner. This is difficult to address directly in cells, but our conclusion is somewhat supported by the finding that downregulation of the two other major topoisomerases with DNA relaxation activity, TOP2α and TOP2β, did not affect $NHEIII_1$ activity in a Pu27 sequence dependent manner. Hence, G4 formation in Pu27 do not appear to be regulated by topology in the utilized test plasmids.

In the present study we demonstrate for the first time that TOP1 can induce G4 formation in double stranded DNA, namely in the Pu27 region of the $NHEIII_1$ promoter, both *in vitro* and in a cellular context. Moreover, we demonstrated that although G4 formation in a naked plasmid depends on negative supercoils, TOP1 was able to overcome such dependence and introduce G4 even in a relaxed DNA fragment. There have been conflicting reports on the effect of TOP1 on G4 formation. Consistent with the present study, a handful of *in vitro* investigations have suggested that TOP1 may influence G4 formation directly by introducing (39) or by binding (36–38) these structures with high affinity. Cellular studies, on the other hand, have demonstrated that TOP1 activity may act as an inhibitor of G4 formation in genomic DNA (46,47) thereby preventing, for example genomic instability induced by G4 (48). This is associated with the relaxation activity of TOP1 that inhibits R-loop formation (24,25) and possibly also by TOP1 attracting G4 resolving RecQ helicases (49,50). Hence, it appears that TOP1 has two counteracting functions when it comes to regulation of G4 formation. It is yet unknown which factors that determine whether TOP1 activity will promote or inhibit G4 formation in a given situation. In the present study, we demonstrated an inhibitory effect of TOP1 on transcription from two G4 forming promoter elements, namely Pu27 and WT21, suggesting a general effect of TOP1 on G4 dependent promoter activity. However, G4 is regulated by a myriad of cis- and trans-acting factors. The specific function of TOP1 may depend on the interplay with these factors, which in turn may be influenced by the physical location and identity of the G4 motif.

SUPPLEMENTARY DATA

Supplementary Data are available at NAR Online.

ACKNOWLEDGEMENTS

We are grateful to Pia M. Martensen, Department of Molecular Biology and Genetics, Aarhus University for kindly providing HEK293T cells and to R. Sternglanz, (State University of New York, Stony Brook, NY) for providing the yeast strain RS190.

Author contribution: J.G.K., K.M.H., R.H. and B.R.K conceived the study. J.G.K., K.M.H., R.H., C.T., A.K.W.S., M.S. and B.R.K designed the experiments. J.G.K., K.M.H. and B.R.K., wrote the manuscript. J.G.K., K.M.H., N.Y.H., A.B.A., A.K.W.S., K.V.P. and M.E.T performed the experiments with the aid of J.U.E., L.L.H., B.S.A. and P.K. All authors have read and agreed to the published version of the manuscript.

FUNDING

Novo Nordisk foundation [0052562]; Independent Research Fund Denmark [8021-000052B]; Fabrikant Einar Willumsens Mindelegat, Familien Erichsens Mindefond, Kleinsmed Helge Arvid Schrøder og hustru Ketty Lydia Larsen Schrøders Fond, Dagmar Marshalls Fond. Funding for open access charge: Familien Erichsens Mindefond.

Conflict of interest statement. None declared.

REFERENCES

1. Kaushik,M., Kaushik,S., Roy,K., Singh,A., Mahendru,S., Kumar,M., Chaudhary,S., Ahmed,S. and Kukreti,S. (2016) A bouquet of DNA structures: emerging diversity. *Biochem. Biophys. Rep.*, **5**, 388–395.
2. Gessner,R.V., Frederick,C.A., Quigley,G.J., Rich,A. and Wang,A.H. (1989) The molecular structure of the left-handed Z-DNA double helix at 1.0-A atomic resolution. Geometry, conformation, and ionic interactions of d(CGCGCG). *J. Biol. Chem.*, **264**, 7921–7935.
3. Chambers,V.S., Marsico,G., Boutell,J.M., Di Antonio,M., Smith,G.P. and Balasubramanian,S. (2015) High-throughput sequencing of DNA G-quadruplex structures in the human genome. *Nat. Biotechnol.*, **33**, 877–881.
4. Hansel-Hertsch,R., Beraldi,D., Lensing,S.V., Marsico,G., Zyner,K., Parry,A., Di Antonio,M., Pike,J., Kimura,H., Narita,M. *et al.* (2016) G-quadruplex structures mark human regulatory chromatin. *Nat. Genet.*, **48**, 1267–1272.
5. Bochman,M.L., Paeschke,K. and Zakian,V.A. (2012) DNA secondary structures: stability and function of G-quadruplex structures. *Nat. Rev. Genet.*, **13**, 770–780.
6. Biffi,G., Tannahill,D., McCafferty,J. and Balasubramanian,S. (2013) Quantitative visualization of DNA G-quadruplex structures in human cells. *Nat. Chem.*, **5**, 182–186.
7. Spiegel,J., Adhikari,S. and Balasubramanian,S. (2020) The structure and function of DNA G-quadruplexes. *Trends Chem.*, **2**, 123–136.
8. Hansel-Hertsch,R., Spiegel,J., Marsico,G., Tannahill,D. and Balasubramanian,S. (2018) Genome-wide mapping of endogenous G-quadruplex DNA structures by chromatin immunoprecipitation and high-throughput sequencing. *Nat. Protoc.*, **13**, 551–564.
9. Yuan,L., Tian,T., Chen,Y., Yan,S., Xing,X., Zhang,Z., Zhai,Q., Xu,L., Wang,S., Weng,X. *et al.* (2013) Existence of G-quadruplex structures in promoter region of oncogenes confirmed by G-quadruplex DNA cross-linking strategy. *Sci. Rep.*, **3**, 1811.

10. Cogoi,S. and Xodo,L.E. (2006) G-quadruplex formation within the promoter of the KRAS proto-oncogene and its effect on transcription. *Nucleic Acids Res.*, **34**, 2536–2549.
11. Palumbo,S.L., Ebbinghaus,S.W. and Hurley,L.H. (2009) Formation of a unique end-to-end stacked pair of G-quadruplexes in the hTERT core promoter with implications for inhibition of telomerase by G-quadruplex-interactive ligands. *J. Am. Chem. Soc.*, **131**, 10878–10891.
12. Siddiqui-Jain,A., Grand,C.L., Bearss,D.J. and Hurley,L.H. (2002) Direct evidence for a G-quadruplex in a promoter region and its targeting with a small molecule to repress c-MYC transcription. *Proc. Natl. Acad. Sci. U.S.A.*, **99**, 11593–11598.
13. Zidanloo,S.G., Colagar,A.H., Ayatollahi,H. and Bagheryan,Z. (2019) G-quadruplex forming region within WT1 promoter is selectively targeted by daunorubicin and mitoxantrone: A possible mechanism for anti-leukemic effect of drugs. *J. Biosci.*, **44**, 12.
14. Marquevielle,J., Robert,C., Lagrabette,O., Wahid,M., Bourdoncle,A., Xodo,L.E., Mergny,J.L. and Salgado,G.F. (2020) Structure of two G-quadruplexes in equilibrium in the KRAS promoter. *Nucleic Acids Res.*, **48**, 9336–9345.
15. Monsen,R.C., DeLeeuw,L., Dean,W.L., Gray,R.D., Sabo,T.M., Chakravarthy,S., Chaires,J.B. and Trent,J.O. (2020) The hTERT core promoter forms three parallel G-quadruplexes. *Nucleic Acids Res.*, **48**, 5720–5734.
16. Felsenstein,K.M., Saunders,L.B., Simmons,J.K., Leon,E., Calabrese,D.R., Zhang,S., Michalowski,A., Gareiss,P., Mock,B.A. and Schneekloth,J.S. Jr (2016) Small molecule microarrays enable the identification of a selective, quadruplex-binding inhibitor of MYC expression. *ACS Chem. Biol.*, **11**, 139–148.
17. Qin,Y. and Hurley,L.H. (2008) Structures, folding patterns, and functions of intramolecular DNA G-quadruplexes found in eukaryotic promoter regions. *Biochimie*, **90**, 1149–1171.
18. Tawani,A., Mishra,S.K. and Kumar,A. (2017) Structural insight for the recognition of G-quadruplex structure at human c-myc promoter sequence by flavonoid Quercetin. *Sci. Rep.*, **7**, 3600.
19. Gonzalez,V., Guo,K., Hurley,L. and Sun,D. (2009) Identification and characterization of nucleolin as a c-myc G-quadruplex-binding protein. *J. Biol. Chem.*, **284**, 23622–23635.
20. Kim,B.G., Shek,Y.L. and Chalikian,T.V. (2013) Polyelectrolyte effects in G-quadruplexes. *Biophys. Chem.*, **184**, 95–100.
21. Sun,D. and Hurley,L.H. (2009) The importance of negative superhelicity in inducing the formation of G-quadruplex and i-motif structures in the c-Myc promoter: implications for drug targeting and control of gene expression. *J. Med. Chem.*, **52**, 2863–2874.
22. Selvam,S., Koirala,D., Yu,Z. and Mao,H. (2014) Quantification of topological coupling between DNA superhelicity and G-quadruplex formation. *J. Am. Chem. Soc.*, **136**, 13967–13970.
23. Zheng,K.W., He,Y.D., Liu,H.H., Li,X.M., Hao,Y.H. and Tan,Z. (2017) Superhelicity constrains a localized and R-loop-dependent formation of G-quadruplexes at the upstream region of transcription. *ACS Chem. Biol.*, **12**, 2609–2618.
24. Huppert,J.L. (2008) Thermodynamic prediction of RNA-DNA duplex-forming regions in the human genome. *Mol. Biosyst.*, **4**, 686–691.
25. Miglietta,G., Russo,M. and Capranico,G. (2020) G-quadruplex-R-loop interactions and the mechanism of anticancer G-quadruplex binders. *Nucleic Acids Res.*, **48**, 11942–11957.
26. Giraldo,R. and Rhodes,D. (1994) The yeast telomere-binding protein RAP1 binds to and promotes the formation of DNA quadruplexes in telomeric DNA. *EMBO J.*, **13**, 2411–2420.
27. Baldrich,E. and O'Sullivan,C.K. (2005) Ability of thrombin to act as molecular chaperone, inducing formation of quadruplex structure of thrombin-binding aptamer. *Anal. Biochem.*, **341**, 194–197.
28. Lago,S., Tosoni,E., Nadai,M., Palumbo,M. and Richter,S.N. (2017) The cellular protein nucleolin preferentially binds long-looped G-quadruplex nucleic acids. *Biochim. Biophys. Acta Gen. Subj.*, **1861**, 1371–1381.
29. Uliel,L., Weisman-Shomer,P., Oren-Jazan,H., Newcomb,T., Loeb,L.A. and Fry,M. (2000) Human Ku antigen tightly binds and stabilizes a tetrahelical form of the Fragile X syndrome d(CGG)n expanded sequence. *J. Biol. Chem.*, **275**, 33134–33141.
30. Mohaghegh,P., Karow,J.K., Brosh,R.M. Jr, Bohr,V.A. and Hickson,I.D. (2001) The Bloom's and Werner's syndrome proteins are DNA structure-specific helicases. *Nucleic Acids Res.*, **29**, 2843–2849.
31. Fry,M. and Loeb,L.A. (1999) Human werner syndrome DNA helicase unwinds tetrahelical structures of the fragile X syndrome repeat sequence d(CGG)n. *J. Biol. Chem.*, **274**, 12797–12802.
32. Sun,H., Bennett,R.J. and Maizels,N. (1999) The *Saccharomyces cerevisiae* Sgs1 helicase efficiently unwinds G-G paired DNAs. *Nucleic Acids Res.*, **27**, 1978–1984.
33. Champoux,J.J. (2001) DNA topoisomerases: structure, function, and mechanism. *Annu. Rev. Biochem.*, **70**, 369–413.
34. Leppard,J.B. and Champoux,J.J. (2005) Human DNA topoisomerase I: relaxation, roles, and damage control. *Chromosoma*, **114**, 75–85.
35. Stewart,L., Redinbo,M.R., Qiu,X., Hol,W.G. and Champoux,J.J. (1998) A model for the mechanism of human topoisomerase I. *Science*, **279**, 1534–1541.
36. Ogloblina,A.M., Bannikova,V.A., Khristich,A.N., Oretskaya,T.S., Yakubovskaya,M.G. and Dolinnaya,N.G. (2015) Parallel G-quadruplexes formed by guanine-rich microsatellite repeats inhibit human topoisomerase I. *Biochemistry (Mosc.)*, **80**, 1026–1038.
37. Marchand,C., Pourquier,P., Laco,G.S., Jing,N. and Pommier,Y. (2002) Interaction of human nuclear topoisomerase I with guanosine quartet-forming and guanosine-rich single-stranded DNA and RNA oligonucleotides. *J. Biol. Chem.*, **277**, 8906–8911.
38. Shuai,L., Deng,M., Zhang,D., Zhou,Y. and Zhou,X. (2010) Quadruplex-duplex motifs as new topoisomerase I inhibitors. *Nucleosides Nucleotides Nucleic Acids*, **29**, 841–853.
39. Arimondo,P.B., Riou,J.F., Mergny,J.L., Tazi,J., Sun,J.S., Garestier,T. and Helene,C. (2000) Interaction of human DNA topoisomerase I with G-quartet structures. *Nucleic Acids Res.*, **28**, 4832–4838.
40. Lisby,M., Krogh,B.O., Boege,F., Westergaard,O. and Knudsen,B.R. (1998) Camptothecins inhibit the utilization of hydrogen peroxide in the ligation step of topoisomerase I catalysis. *Biochemistry*, **37**, 10815–10827.
41. Brooks,T.A. and Hurley,L.H. (2009) The role of supercoiling in transcriptional control of MYC and its importance in molecular therapeutics. *Nat. Rev. Cancer*, **9**, 849–861.
42. Zidanloo,S.G., Hosseinzadeh Colagar,A., Ayatollahi,H. and Raoof,J.B. (2016) Downregulation of the WT1 gene expression via TMPyP4 stabilization of promoter G-quadruplexes in leukemia cells. *Tumour Biol.*, **37**, 9967–9977.
43. Brazda,V., Kolomaznik,J., Lysek,J., Bartas,M., Fojta,M., Stastny,J. and Mergny,J.L. (2019) G4Hunter web application: a web server for G-quadruplex prediction. *Bioinformatics*, **35**, 3493–3495.
44. Lee,J.H. and Berger,J.M. (2019) Cell cycle-dependent control and roles of DNA topoisomerase II. *Genes (Basel)*, **10**, 859.
45. Riou,J.F., Vilarem,M.J., Larsen,C.J. and Riou,G. (1986) Characterization of the topoisomerase II-induced cleavage sites in the c-myc proto-oncogene. In vitro stimulation by the antitumoral intercalating drug mAMSA. *Biochem. Pharmacol.*, **35**, 4409–4413.
46. Berroyer,A. and Kim,N. (2020) The functional consequences of eukaryotic topoisomerase 1 interaction with G-quadruplex DNA. *Genes (Basel)*, **11**, 193.
47. Kim,N. (2019) The interplay between G-quadruplex and transcription. *Curr. Med. Chem.*, **26**, 2898–2917.
48. Maizels,N. (2015) G4-associated human diseases. *EMBO Rep.*, **16**, 910–922.
49. Laine,J.P., Opresko,P.L., Indig,F.E., Harrigan,J.A., von Kobbe,C. and Bohr,V.A. (2003) Werner protein stimulates topoisomerase I DNA relaxation activity. *Cancer Res.*, **63**, 7136–7146.
50. Lebel,M., Spillare,E.A., Harris,C.C. and Leder,P. (1999) The Werner syndrome gene product co-purifies with the DNA replication complex and interacts with PCNA and topoisomerase I. *J. Biol. Chem.*, **274**, 37795–37799.